

# Reduction of N<sub>2</sub>O in a circulating fluidized-bed combustor

Lars-Erik Åmand and Bo Leckner

Chalmers University of Technology, Department of Energy Conversion,  
S-412 96 Göteborg, Sweden

(Received 25 June 1993; revised 26 September 1993)

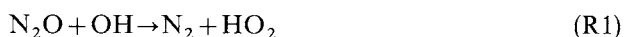
Nitrous oxide was injected at various locations in the combustion chamber of a circulating fluidized-bed boiler during combustion of fuels of different volatiles matter: coke, bituminous coal and wood. The reduction of the N<sub>2</sub>O injected was measured and the results were compared with calculations using available kinetic data. The reduction of the N<sub>2</sub>O introduced into the lower part of the combustion chamber was >80%, but also, especially in wood combustion, at the top of the combustion chamber a certain degree of reduction occurred, which is interpreted as being caused by volatiles combustion. The available kinetic data are still not sufficiently accurate for definite conclusions from calculations.

(Keywords: nitrous oxide; reduction; fluidized-bed combustion)

The formation and destruction of N<sub>2</sub>O during combustion have been described in recent surveys<sup>1-4</sup>, where it has been stated that fluidized-bed combustion (FBC) is one of the few combustion methods yielding a considerable emission (50–200 ppmv) of N<sub>2</sub>O. The present paper focuses on the mechanisms of destruction of N<sub>2</sub>O in a circulating fluidized-bed (CFB) boiler and in particular on the question of whether the destruction is dominated by homogeneous gas-phase reactions or by heterogeneous gas–solid or solid-catalysed reactions. The mechanisms of N<sub>2</sub>O formation in a CFB boiler have been studied in parallel with the present project, but the results are reported separately<sup>5</sup>.

## HOMOGENEOUS AND HETEROGENEOUS REDUCTION OF N<sub>2</sub>O

The principal homogeneous and heterogeneous mechanisms of N<sub>2</sub>O destruction have been studied in laboratory experiments and with sensitivity analyses using kinetic schemes. On the basis of the comprehensive scheme of homogeneous reaction kinetics of Miller and Bowman<sup>6</sup>, Kramlich *et al.*<sup>7</sup> and Kilpinen and Hupa<sup>8</sup> have identified the following reactions as important for the homogeneous destruction of N<sub>2</sub>O under FBC conditions:



In the absence of radicals, thermal decomposition may also play a role:



M is a 'third body', which in a boiler is N<sub>2</sub>, CO<sub>2</sub> and O<sub>2</sub>.

Laboratory studies of thermal decomposition have been carried out by Hulgaard<sup>9,10</sup> and continued by Johnsson *et al.*<sup>11</sup>. Iisa *et al.*<sup>12</sup> and Miettinen *et al.*<sup>13</sup> also reported results concerning thermal decomposition of N<sub>2</sub>O. The differences in the results reported in the literature on reaction (R3) are explained by Johnsson *et al.*<sup>11</sup> as being due to an effect of the different carrier gases used (helium, argon or nitrogen) in the reactor experiments. Hulgaard<sup>10</sup> added CO and found an increase in N<sub>2</sub>O reduction at lower temperatures. This was interpreted as being an effect of reaction (R1). Iisa *et al.*<sup>12</sup> used carrier gases with different water contents and found a slight increase in N<sub>2</sub>O reduction when water was added. This result could also be an effect of reactions (R1) and (R2). Aho *et al.*<sup>14</sup> observed a large reduction of N<sub>2</sub>O in their experiments in an entrained flow reactor burning peat at low excess air ratios which, according to the authors, favoured reactions (R1) and (R2).

In addition to the homogeneous reduction of N<sub>2</sub>O by reactions (R1) to (R3), various solid surfaces are known to catalyse N<sub>2</sub>O reduction in the temperature range of interest for FBC. The effect of char on the N<sub>2</sub>O reduction has been studied by a number of workers<sup>15-19</sup>. Inorganic materials such as CaO, CaSO<sub>4</sub>, MgO, SiO<sub>2</sub>, Fe<sub>2</sub>O<sub>3</sub> and Fe<sub>3</sub>O<sub>4</sub> have been studied to a certain extent<sup>13-15,20-25</sup>. Attempts to compare the results from the various laboratory studies have been made by de Soete<sup>25</sup> and Johnsson<sup>26</sup>. They both constructed Arrhenius plots based on the assumption of first-order reactions and plug flow in the various laboratory reactors. In the comparison made by de Soete the char material is the most reactive and silica sand is the most inert solid. CaO is more reactive than CaSO<sub>4</sub>. The high catalytic activity of CaO is not simply an effect of its greater internal surface area<sup>13,21</sup>, but the internal surface area has to be considered when comparing different materials<sup>21</sup>. Some materials, such as Fe<sub>3</sub>O<sub>4</sub> (magnetite), do not act as catalysts; instead, Fe<sub>3</sub>O<sub>4</sub> is oxidized to Fe<sub>2</sub>O<sub>3</sub> (hematite),

Presented at 'NO<sub>x</sub>: Basic Mechanisms of Formation and Destruction, and their Application to Emission Control Technologies', 20–22 April 1993, London, UK

**Table 1** First-order rate constants for decomposition of N<sub>2</sub>O on surfaces and thermal decomposition in N<sub>2</sub><sup>a</sup>

	$k_0$	$E/R$ (K)	$k$ (1123 K)	Experimental data from ref.
Quartz sand, analytical grade	0.056 <sup>b</sup>	4650	0.00089 <sup>b</sup>	20
Quartz sand, analytical grade	8.3 <sup>b</sup>	10 000	0.0011 <sup>b</sup>	13
FBC bed material (Pechora coal)	$6.4 \times 10^{5b}$	21 400	0.0034 <sup>b</sup>	20
Peat ash	$5.3 \times 10^{8b}$	25 650	0.064 <sup>b</sup>	20
Cedar Grove char	267 <sup>c</sup>	13 900	1.3 <sup>b</sup>	15
Prosper char	201 <sup>c</sup>	12 200	4.3 <sup>b</sup>	15
Eschweiler char	41.6 <sup>c</sup>	10 000	6.3 <sup>b</sup>	15
Thermal decomposition in N <sub>2</sub>	$4.2 \times 10^{9d}$	27 000	0.15 <sup>d</sup>	11

<sup>a</sup> Adapted from ref. 26;  $k = k_0 \exp(-E/RT)$ , except for char, where  $k \cong k_0 T \exp(-E/RT)$

<sup>b</sup> m<sup>3</sup> kg<sup>-1</sup> s<sup>-1</sup>

<sup>c</sup> m<sup>3</sup> kg<sup>-1</sup> s<sup>-1</sup> K<sup>-1</sup>

<sup>d</sup> s<sup>-1</sup>

which gives an extremely high reduction of N<sub>2</sub>O even at low temperatures (600°C)<sup>13</sup>.

Some of the results referred to are expressed as reaction rate constants, which can be used to calculate N<sub>2</sub>O reduction in a certain application. Table 1 presents examples of rate constants for reduction of N<sub>2</sub>O on char, quartz sand, one bed material sample and one sample of peat ash.

Knowledge on N<sub>2</sub>O destruction is increasing, although there are still differences in the data from various investigations. A further problem remains: to translate this knowledge obtained in laboratory investigations to combustors. This is not readily done, since the complexity of combustion chambers impedes a straightforward application of laboratory results. For instance, the question of whether the reduction of N<sub>2</sub>O is caused by homogeneous or heterogeneous reactions has not yet been answered. The present investigation is aimed at providing some answers to these questions by a study of N<sub>2</sub>O reduction in a CFB boiler during combustion of three fuels of widely different volatile matter.

## EXPERIMENTAL

### Boiler

The tests were run in the 12 MW(th) CFB boiler at Chalmers University of Technology (Figure 1). The boiler is built in the form of a commercial unit with a combustion chamber made up of membrane tube walls with a height of 13.5 m and a cross-section of about 2.9 m<sup>2</sup>. Fuel is fed to the bottom of the combustion chamber through a fuel chute (1). The bed material entrained is separated from the gases in the hot cyclone (2) and passed back to the combustion chamber through the return leg and particle seal (4). Primary air is introduced through nozzles in the bottom plate (5), and secondary air can be injected through several inlets, consisting of sets of nozzles located along the combustion chamber at various heights as indicated by arrows in Figure 1. The lowest secondary air inlet (6) is located at 2.2 m, the second (7) at 3.8 m and the third and highest (8) at 5.5 m. Secondary air can also be introduced to the entrance of the hot cyclone (9). In the present tests only the lowest inlet at 2.2 m was used. The inlet at 5.5 m and at the entrance of the cyclone

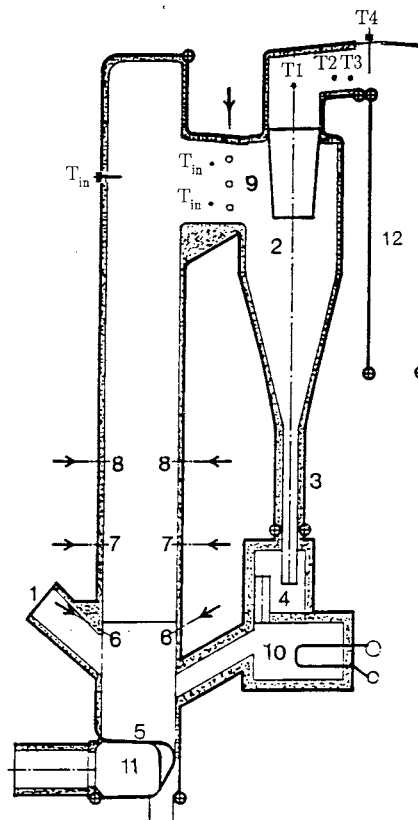


**Figure 1** Diagram of the 12 MW CFB boiler at Chalmers University of Technology. 1, Fuel feed chute; 2, cyclone; 3, particle return leg; 4, particle seal; 5, bottom plate; 6, secondary air inlet at 2.2 m; 7, secondary air inlet at 3.8 m; 8, secondary air inlet at 5.5 m; 9, secondary air inlet in the duct to the cyclone; 10, heat exchanger; 11, air plenum; 12, convection section; T, thermocouples

can also be supplied with recycled flue gas, used as carrier gas for the concentrated N<sub>2</sub>O which was injected into the combustion chamber.

The bed temperature is controlled by a heat exchanger (10) located in communication with the particle seal and by recycled flue gas which is mixed with the primary air in the air plenum (11) before entering the combustion chamber. Figure 1 also shows the location of thermocouples at the top of the combustion chamber as well as in the exit duct of the cyclone; they were important for the determination of the reaction environment when N<sub>2</sub>O was supplied to the cyclone.

### Measurements

Data needed for the evaluation procedure were collected with a data-acquisition system. The concentrations of O<sub>2</sub>, NO, N<sub>2</sub>O and CO were measured in the stack with continuous gas analysers. A chemiluminescence analyser was used for NO, a non-dispersive infrared analyser for N<sub>2</sub>O and CO, and a paramagnetic analyser for O<sub>2</sub>. The N<sub>2</sub>O analyser is cross-sensitive towards methane (CH<sub>4</sub>). Also, a disturbance from SO<sub>2</sub> at concentrations > 500 ppmv can cause a problem, but this level of SO<sub>2</sub> was not reached, owing to the low sulfur content of the fuels used. During normal operation, CH<sub>4</sub> is not present in the flue gases leaving the boiler. This was also the case during combustion of wood chips, according to regular checks with an on-line total hydrocarbon analyser. Gas was sampled at two locations in the combustion chamber in addition to the

measurement in the stack. Gas was withdrawn through a cooled filter located at the end of each of two probes, and the particle-free gas was analysed on-line for O<sub>2</sub>, CO, NO and total hydrocarbons. Gas from the probes was also collected (after drying) in Tedlar bags for further analyses of N<sub>2</sub>O, H<sub>2</sub> and hydrocarbons on three gas chromatographs equipped with different columns and detectors: a thermal conductivity detector for H<sub>2</sub>, an electron capture detector for N<sub>2</sub>O, and a flame ionization detector for hydrocarbons.

**Table 2** Fuel characteristics

	Wood chips	Bituminous coal <sup>a</sup>		Coke
		A	B	
Particle size				
Mass mean (mm)	9.6	6.0	not analysed	2.5
<1 mm (%)	0.0	28.5	not analysed	54.5
Volatiles (wt% daf)	78.0	39.9	28.2	3.4
Proximate analysis (wt% a.r.)				
Combustibles	71.1	78.6	88.6	79.5
Ash	0.2	6.6	6.7	9.8
Moisture	28.7	14.8	4.7	10.7
Ultimate analysis (wt% daf)				
C	50.6	79.8	86.9	96.1
H	6.2	5.3	5.2	0.7
O	43.0	12.6	5.6	1.2
S	0.02	0.7	0.8	0.7
N	0.14	1.6	1.5	1.3

<sup>a</sup>As used in 12 MW CFB boiler (A) and for coke production (B)

**Table 3** Solids and char contents (kg) in the combustion chamber

Location from bottom (m)	Wood chips		Bituminous coal		Coke	
	0-2.3	2.3-13	0-2.3	2.3-13	0-2.3	2.3-13
Solids	1160	290	1040	310	1540	580
Char	1.3	0.3	22.4	3.1	184	45.2

**Table 4** Concentrations of reducing species (ppmv) and oxygen (vol.%) at two locations in the combustion chamber

Location from bottom (m)	Wood chips		Bituminous coal		Coke	
	2.5	11.0	2.5	11.0	2.5	11.0
O <sub>2</sub>	3.04	1.75	4.04	4.38	2.31	4.82
CO	35 900	15 100	9000	1200	12 900	340
H <sub>2</sub>	14 200	6500	2100	60	80	BDL <sup>d</sup>
CH <sub>4</sub>	4900	2000	1000	20	6	1
C <sub>2</sub> H <sub>6</sub>	400	300	50	1	BDL	BDL
C <sub>2</sub> H <sub>4</sub>	2000	500	400	7	1	BDL
C <sub>2</sub> H <sub>2</sub>	200	30	65	0.5	BDL	BDL
∑ C <sub>3</sub>	200	15	50	BDL	BDL	BDL
∑ C <sub>4</sub>	100	10	BDL	BDL	BDL	BDL
∑ C <sub>5</sub>	10	BDL	BDL	BDL	BDL	BDL
∑ HC <sup>a</sup>	7700	2900	1600	30	7	1
∑ HC <sup>b</sup>	6100	1900	1800	50	20	3
∑ RS <sup>c</sup>	57 800	24 500	12 700	1290	13 000	340

<sup>a</sup>Total hydrocarbon concentration based on gas chromatographic analysis

<sup>b</sup>Total hydrocarbon concentration based on on-line analyser

<sup>c</sup>Total concentration of reducing species (CO, H<sub>2</sub>, C<sub>1</sub>-C<sub>5</sub> hydrocarbons)

<sup>d</sup>Below detection limit (0.5 ppmv for hydrocarbons, 50 ppmv for H<sub>2</sub>)

## Fuels

The reference fuel was a bituminous coal from Colombia. In addition, high-volatile wood chips and low-volatile coke were chosen for comparison. The wood chips were produced for research purposes out of dried pieces of pine (waste from furniture and house construction). The coke, normally used in the steel industry, was produced at the Oxelösund coking plant, Sweden, from a blend of eight commercial imported bituminous coals. The residual volatile matter was only 3.4 wt% (daf). The fuel analyses are given in Table 2. The three fuels burned differently in the CFB boiler. The coke burned slowly because of its low reactivity, which led to accumulation of large quantities of char in the combustion chamber; on the other hand, the concentration of hydrocarbons in the combustion chamber was very low. The wood chips behaved in the opposite way: there was almost no accumulation of char, but the concentration of hydrocarbons (and hydrogen) was very high. The bituminous coal showed intermediate values. The char content in the combustion chamber is shown in Table 3, and the corresponding hydrocarbon content in Table 4. Table 3 is based on bed density measurements by pressure drops and on char samples taken over the height of the combustion chamber, and Table 4 on measurements with the gas sampling probes. The samples were taken in the centre of the combustion chamber.

## Test programme

The boiler was operated with all three fuels under reference conditions, the most important of which were: a bottom bed temperature of 850°C, an excess-air ratio of 1.20-1.25, and a ratio of primary to secondary air corresponding to a calculated primary-air stoichiometry of 0.70-0.75. The calculated primary-air stoichiometry expresses the ratio of primary-air feed rate to the stoichiometric air requirement corresponding to the fuel feed rate. This definition presupposes that all fuel burns below the secondary-air inlet, but this is not actually the case. The actual excess air in the bottom

zone below the secondary-air inlet is therefore  $>0.75$  and also depends on the type of fuel.

The boiler load was maintained at about 8 MW during all tests. With the air ratio chosen, this load gives a fluidization velocity of about  $5 \text{ m s}^{-1}$  at the top of the combustion chamber. Since calcined lime is known to influence the formation of  $N_2O$  as well as to catalyse its decomposition<sup>12,13,21,22,24,25,27</sup>, the tests were carried out without lime addition. The bed consisted of commercial silica sand mixed with some fuel ash and char from the combustion of the various fuels.

#### $N_2O$ injection

In order to study the reduction of  $N_2O$  in the fluidized bed,  $N_2O$  was introduced to the combustion chamber at three locations: the primary-air duct, the secondary-air inlet at 5.5 m and the entrance of the cyclone (positions 11, 8 and 9 respectively in *Figure 1*).

At room temperature and normal pressure,  $N_2O$  is a gas, but it is stored as a liquid in steel cylinders at elevated pressures. During the present tests, liquid  $N_2O$  was first evaporated in a heat exchanger and then, after passing a rotameter, it was injected as a gas, either into the primary air at location 11 or into a recirculated flue gas stream directed to the secondary-air nozzles at 5.5 m or to the entrance of the cyclone. The flow rate of the recirculated flue gas as carrier gas was a compromise between the requirement of an even distribution of  $N_2O$  over the combustion chamber cross-section and the avoidance of local cooling of the medium in the combustion chamber.

The  $N_2O$  cylinder was weighed continuously during an injection test and the flow of  $N_2O$  was subsequently calculated. The position of the rotameter throttle required for a stable flow of  $N_2O$  was determined in preliminary tests.

#### Temperature control

$N_2O$  reduction depends on temperature. Therefore it is desirable to maintain a constant temperature in the combustion chamber, which is feasible at the load chosen. However, minor temperature variations occur and have to be considered. *Figure 2* shows the temperature profile in the combustion chamber, cyclone and cyclone exit duct. The temperature at the bottom of the combustion chamber was always maintained at  $850^\circ\text{C}$  by the control system. With wood and coke there was more combustion in the top part of the combustion chamber than with bituminous coal. During combustion of wood chips the volatiles were responsible for the temperature rise in the top of the combustion chamber seen in *Figure 2*, whereas with coke the temperature rise was caused by combustion of accumulated char (*Table 3*). In the cyclone, the temperature fell owing to cooling by the walls of the cyclone. The temperature drop was smaller with wood chips because of the combustion of greater quantities of CO, hydrocarbons and hydrogen in the cyclone (see *Table 4*) than with the other fuels.

In the cyclone exit duct there was a further fall in temperature. This temperature is represented by an average of the three thermocouples T2, T3 and T4 (*Figure 1*). These thermocouples show almost the same temperature, but unfortunately they are all affected by the cold walls of the boiler convection section. This means that the temperature drop in the cyclone exit duct is 20–30 K less than that shown in *Figure 2*.

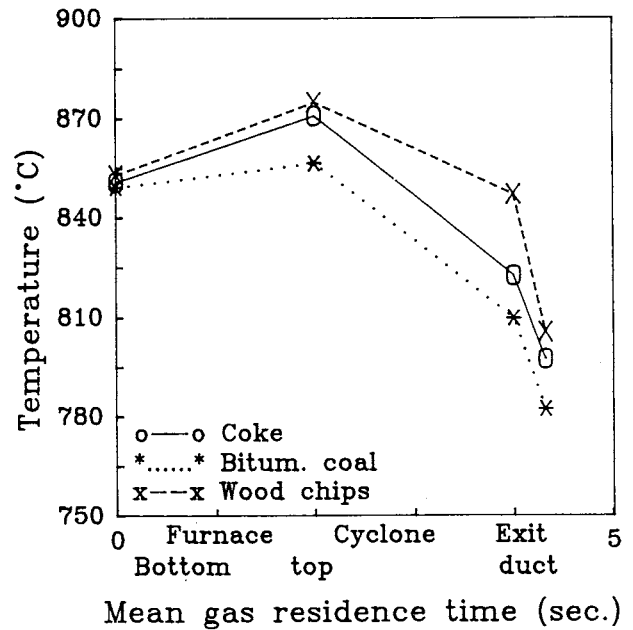


**Figure 2** Temperature profiles along gas path from bottom of combustion chamber to entrance to convection section for the three fuels. The two sets of temperatures shown for the exit duct are those of the cyclone outlet (T1) and an average of T2, T3 and T4 (of *Figure 1*)

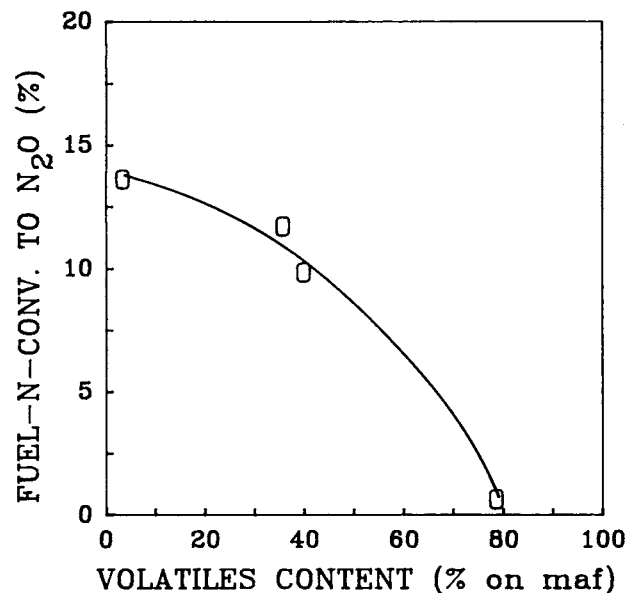


**Figure 3** Conversion of fuel-N to  $N_2O$  as a function of volatile matter of fuel. Reference operating conditions. Fuels: see *Table 2* and ref. 28

## RESULTS

#### Reference conditions

The conversion of the fuel-nitrogen to  $N_2O$  from the three fuels in the reference case is presented in *Figure 3* together with the result from operation with another bituminous coal under identical conditions in a previous project on the boiler<sup>28</sup>. The graph shows that a low-volatile fuel, such as coke, led to the highest conversion, whereas high-volatile fuels such as wood gave almost no emission of  $N_2O$ .

#### $N_2O$ injection tests

*Figure 4* shows the result of  $N_2O$  injection into the primary air duct with bituminous coal as a fuel.  $N_2O$

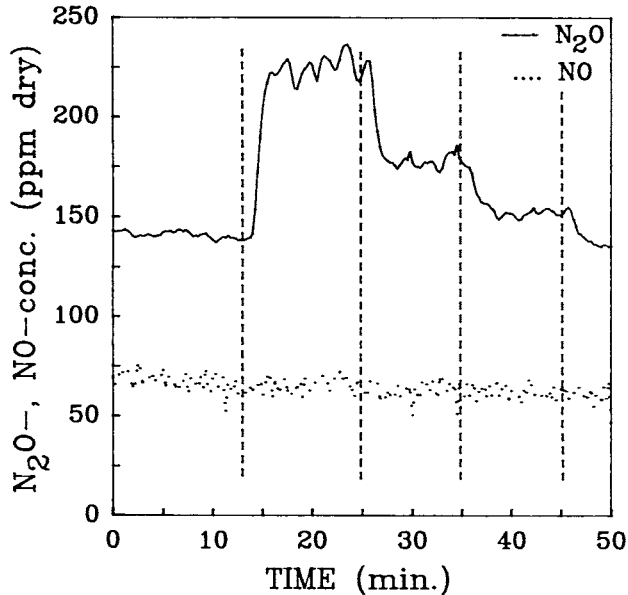


Figure 4  $N_2O$  and NO concentrations in stack gas resulting from injection of  $N_2O$  into the primary air duct in three steps at concentrations of 1010, 500 and 250 ppmv in the time intervals 13–25, 25–35 and 35–45 min respectively. Reference operating conditions. Fuel: bituminous coal

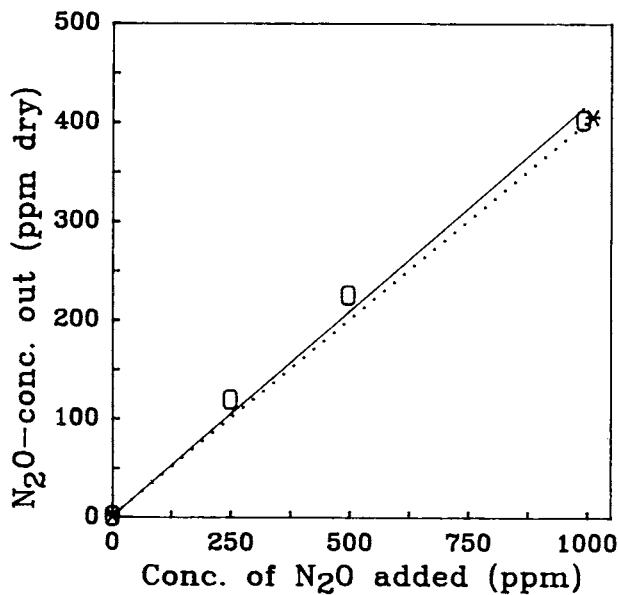


Figure 5 Comparison of  $N_2O$  concentrations in stack gas in two independent tests with  $N_2O$  injected at the 5.5 m level:  $\circ$ , main test; \*, preliminary test. Reference operating conditions. Fuel: wood chips

was supplied in three steps, in concentrations of 1010, 500, and 250 ppmv  $N_2O$  relative to the entire flow of air supplied to the boiler. A clear rise in the  $N_2O$  concentration in the stack was observed, but the NO concentration remained constant. No effect on NO emission was recorded in any of the  $N_2O$  injection tests, regardless of fuel or level of injection.

If  $N_2O$  emission is plotted against amount of  $N_2O$  injected, a straight-line relation is obtained. An example from operation with wood chips and  $N_2O$  injection at the 5.5 m level is shown in Figure 5, which also contains a line from the preliminary test. The good agreement between these lines in this and similar tests verifies the

accuracy of the test procedure. This is especially important, since the preliminary and main tests were run on different occasions with other fuels and other boiler operating conditions intervening, and the reference conditions had to be re-established before the main test was conducted.

In Figure 6 the data of Figure 4 are compared with those of the other fuels for tests with  $N_2O$  injection into the primary-air duct. With coke as fuel, the reduction of  $N_2O$  was less than that found with bituminous coal (the line has a greater slope). On the other hand, the combustion of wood led to a much greater reduction of  $N_2O$  than that of the other fuels. Similar straight-line fits with high correlation coefficients ( $\geq 0.95$ ) represent the other injection tests as well, and the lines can be used to calculate  $N_2O$  reduction. All the results can be shown in this form in a single plot, Figure 7, which expresses the reduction of  $N_2O$  as a function of height of injection into the combustion chamber. The trends shown in Figure 7 can be summarized thus:

- (1) reduction of  $N_2O$  was very strong in the dense bottom bed of the combustion chamber, and was always  $> 80\%$  when the gas was injected with the primary air to the bottom of the combustion chamber;
- (2) reduction was less in the top of the combustion chamber than in the bottom, but it was still considerable, especially in the case of wood combustion;
- (3) the high-volatile-low-char extreme of wood combustion showed a much greater reduction of  $N_2O$  than the other, low-volatile-high-char, extreme of coke combustion.

#### Calculation of $N_2O$ reduction

Is it possible to represent the results of Figure 7 by means of available laboratory data on  $N_2O$  reduction? The amount of bed material and its composition are known, so the contribution to reduction by the bed material can be estimated. However, the contribution to reduction by radicals cannot be calculated, since

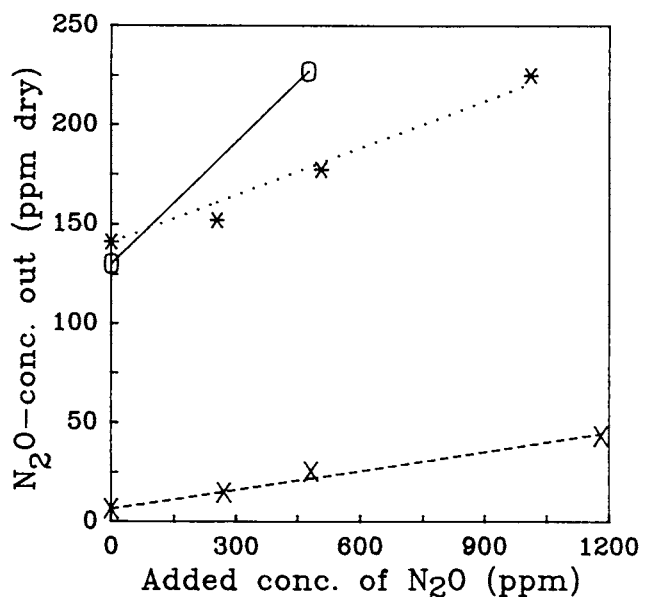


Figure 6 Concentration of  $N_2O$  in stack gas as a function of concentration of  $N_2O$  injected into primary air duct for the three fuels:  $\circ$ , coke; \*, bituminous coal;  $\times$ , wood chips. Reference operating conditions

Table 5 Input data used in model calculation

Section of boiler Location	I 0-2.3 m	II 2.3-5.5 m	III 5.5-13 m	IV Cyclone	V Cyclone outlet
Char content, $m_{char}$ (kg m <sup>-3</sup> )	4.18	0.151	0.0814	0.0020	0.0020
Solids (inert) content, $m_{bed}$ (kg m <sup>-3</sup> )	190	14.8	7.96	0.0025	0.0025
Flow of gas, $V_0$ (m <sup>3</sup> s <sup>-1</sup> )	9.02	14.3	15.0	14.8	14.4
Volume of combustor section, $V$ (m <sup>3</sup> )	5.37	9.25	21.7	8.9	2.4
Temperature (K)	1123	1123	1123	1108	1078

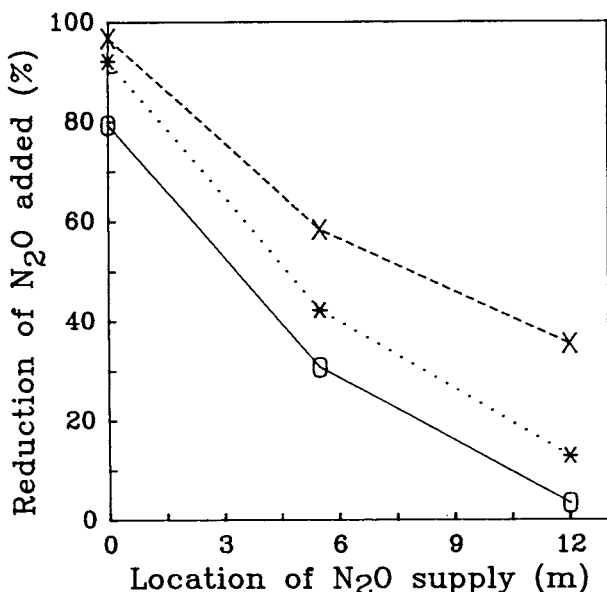


Figure 7 Reduction of injected N<sub>2</sub>O as a function of injection distance from bottom of combustion chamber. Symbols as in Figure 6. Reference operating conditions

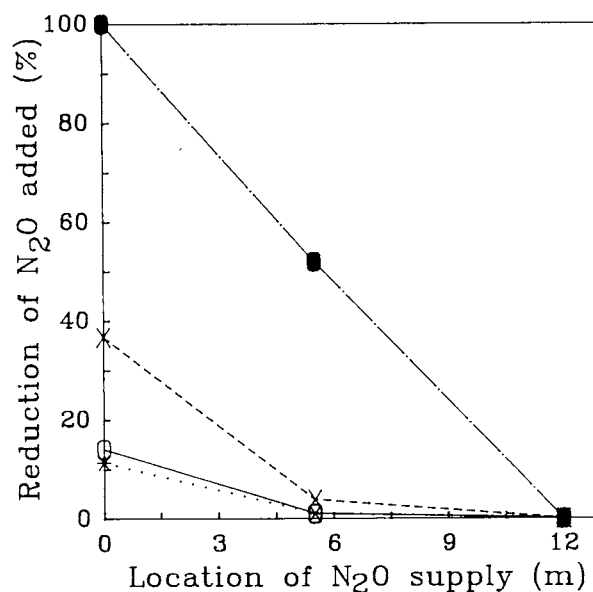


Figure 8 Calculated reduction of injected N<sub>2</sub>O as a function of injection distance for different bed materials: \*, quartz sand, analytical grade (refs 12, 20); ○, quartz sand, analytical grade (ref. 13); ×, FBC bed material from coal combustion without lime addition (ref. 20); ●, peat ash (1.2 wt% combustibles) (refs 12, 20)

the radical concentration in the highly particle-laden atmosphere of the combustor is unknown. However, the thermal decomposition can be calculated, and, together with the contribution of particles, the N<sub>2</sub>O reduction can be estimated, assuming plug flow:

$$dC_{N_2O}/dV = -r_{N_2O}/V_0 \quad (1)$$

$$-r_{N_2O} = (k_{N_2} + k_{bed}m_{bed} + k_{char}m_{char})C_{N_2O} \quad (2)$$

where  $C_{N_2O}$  = concentration of N<sub>2</sub>O (kmol m<sup>-3</sup>),  $V_0$  = volume flow of gas at bed temperature (m<sup>3</sup> s<sup>-1</sup>),  $dV$  = volume element of combustion chamber (m<sup>3</sup>),  $r_{N_2O}$  = rate of N<sub>2</sub>O reduction (kmol m<sup>-3</sup> s<sup>-1</sup>),  $k_{N_2}$  = reaction rate constant for reaction (R3) (s<sup>-1</sup>),  $k_{bed}$ ,  $k_{char}$  = reaction rate constants for the solid-catalysed N<sub>2</sub>O decomposition on bed material and char respectively (m<sup>3</sup> kg<sup>-1</sup> s<sup>-1</sup>), and  $m_{bed}$ ,  $m_{char}$  = concentrations of inert bed material and char respectively (kg m<sup>-3</sup>).

First-order reactions with respect to N<sub>2</sub>O are assumed in Equation (2). Equation (1) is integrated in five steps over the combustion chamber and cyclone, considering the locations of supply of secondary air and N<sub>2</sub>O and the temperature pattern given in Figure 2. The bed consists of silica sand and char. Data from the run with bituminous coal, given in Table 5, were used in the calculations. Reaction rates of bed material and char were

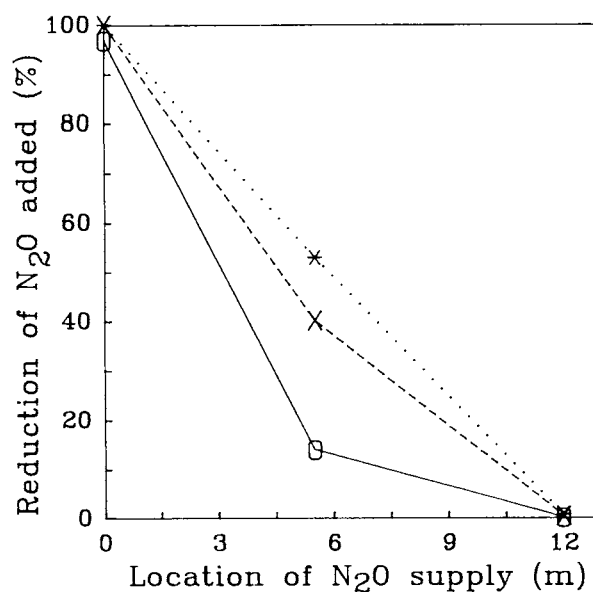
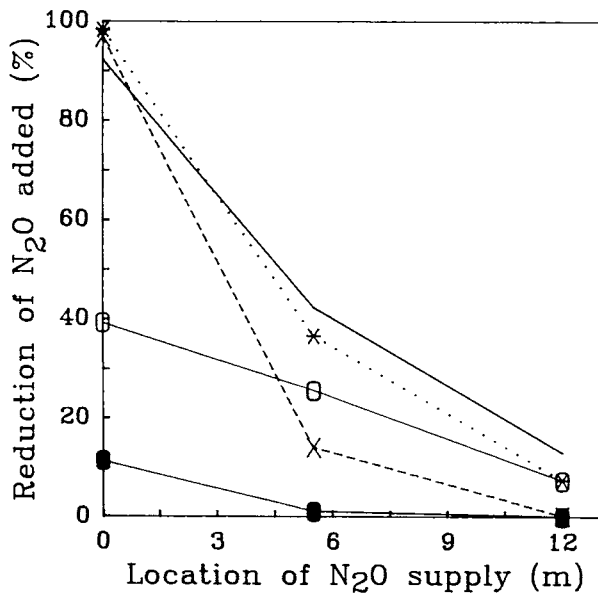


Figure 9 Calculated reduction of injected N<sub>2</sub>O as a function of injection distance for different bituminous coal chars (ref. 15): ○, Cedar Grove; ×, Prosper; \*, Eschweiler

taken from the compilation of data by Johnson<sup>26</sup>. The reaction rate constant for the decomposition reaction (R3) is given by Johnson *et al.*<sup>11</sup>. All the kinetic data used are given in *Table 1*. The results of the calculation are shown in *Figures 8–10*.

In *Figure 8*, the reductions of N<sub>2</sub>O by bed materials with different reactivities are compared. Pure quartz particles are rather inert, but peat ash or bed material taken from a fluidized bed burning coal is far more reactive. A very high reduction by the peat ash is observed. In *Figure 9*, three different chars are compared using kinetic data originally obtained by de Soete<sup>15</sup>. Suzuki *et al.*<sup>17</sup> determined the reactivity of another char and found the same order of magnitude as measured by de Soete. All the chars in *Figure 9* result in almost complete reduction when N<sub>2</sub>O is added to the bottom of the



**Figure 10** Comparison between calculated and measured reduction of injected N<sub>2</sub>O as a function of injection distance. Calculated: ●, quartz sand (refs 12, 20); ×, Cedar Grove char (ref. 15); ○, thermal decomposition (ref. 11); \*, resulting reduction assuming parallel reactions. Measured: upper solid line, bituminous coal (from *Figure 7*)

combustion chamber. Since the char at the bottom of the bed consists predominantly of 1–2 mm particles, and the laboratory data are for much smaller particles (35–50 μm), mass transfer limitation may lower the actual reduction rate of the char-catalysed reaction in this part of the bed.

*Figure 10* is a summary plot. Results from the calculation with pure quartz, one char and the thermal decomposition reaction (R3) are plotted separately. Also plotted is the result when the process is considered as a set of parallel reactions, and the calculations are compared with the measured N<sub>2</sub>O reduction during combustion of bituminous coal (*Figure 7*). The significance of the fairly good agreement between the calculated reduction by the set of parallel reduction reactions and the measured N<sub>2</sub>O reduction during combustion of bituminous coal should not be exaggerated: the char which gave the best fit, Cedar Grove, was chosen from the three chars in *Figure 9* for the comparison.

*Figures 8–10* illustrate the consequence of the wide scatter of kinetic data, which makes definite conclusions impossible. However, if reduction on solids is important, as the data sets indicate, the solids contribute significantly to reduction in the bottom part of the bed where most of the solids are present, whereas in the top part of the combustor there is a gap between measured and calculated values. This gap is most probably due to the contribution of radicals from volatiles combustion to N<sub>2</sub>O reduction.

## DISCUSSION

### Reference conditions

*Figure 3* shows that the emission characteristics of N<sub>2</sub>O strongly depend on the type of fuel, here represented by the volatile matter. The differences in nitrogen content between the fuels are compensated for by expressing the emission in terms of conversion of fuel-nitrogen. The trend shown in *Figure 3* is also supported by results from other CFB reactors of different size, under the conditions listed in *Table 6*, as illustrated in *Figure 11*. A similar dependence on volatile matter has also been found for a small bubbling fluidized bed<sup>31</sup>.

**Table 6** Conditions of tests relating to *Figure 11*

Reference	This work	29	1	30
Data points	A	B	C	D
Bed temp. (°C)	850	850	830–875	850
Excess air ratio	1.2–1.25	1.2–1.25	unknown	1.4–1.5
Primary-air stoichiometry	0.7–0.75	0.7–0.75	unknown	unknown
Bed area (m <sup>2</sup> )	2.9	1.8	0.20	0.008
Furnace height (m)	13.5	8.5	12.8	5.0
Ca/S ratio	0	0	0	0
Fuels used <sup>a</sup>	Coke (2.5)	Pet. coke (14.4)	Bitum. coal (39.5)	Idemitsu-B coal (30.9)
	Bitum. coal (35.7)	Bitum. coal (35.5)	Subbitum. coal (42.0)	Datong coal (33.1)
	Bitum. coal (39.9)	Bitum. coal (35.5)	Lignite (50.7)	Taiheiyo coal (54.8)
	Wood chips (78.0)	Brown coal (53.1)		

<sup>a</sup>Figures in parentheses are volatile matter (wt% daf)

This dependence of N<sub>2</sub>O emission on fuel type has been explained<sup>1,3,32</sup> as being an effect of fuel-nitrogen functionality on the formation of N<sub>2</sub>O. However, emission is the net effect of formation and destruction. The present data show that the reduction reactions also have to be considered if N<sub>2</sub>O emission results from combustion of fuels of different types are to be explained. The volatile matter of the fuel and the resulting carbon monoxide, hydrocarbons and hydrogen, which are likely to produce radicals for N<sub>2</sub>O reduction by reactions (R1) and (R2), are important factors that need to be further considered.

*N<sub>2</sub>O injection tests*

Available data for calculation of N<sub>2</sub>O reduction do not give a reliable prediction. The reductions calculated in Figure 9 for bituminous coal have a wide spread, depending on the data set used. The data chosen for comparison with the measurements in the boiler, Figure 10, resulted in a reasonably good agreement, but the data for the other chars in Figure 9 would have given higher reductions than the measured ones, at least in the bottom and central parts of the combustor. This discrepancy between measured and calculated results would have been even greater in the case of coke, with its higher char concentrations. In addition to the uncertainty about the reactivity of chars, the bed material may play a considerable role if it consists of ash of high reactivity such as that of the peat shown in Figure 8. However, this is probably an extreme case, and although more information is needed on this subject, it may be suspected that the result obtained by Santala *et al.*<sup>20</sup> represents the activity of a normal FBC bed material without lime and char.

The principal uncertainty in the calculation lies not only in the reactivity of different chars but also in lack of knowledge of char pore structure and particle size distribution in various locations of the bed. In the present calculations the efficiency factor of the reduction reaction was simply assumed to be unity, i.e. the same efficiency factor that was implicitly used in the results of the laboratory tests, which were related to kg of char per m<sup>3</sup>

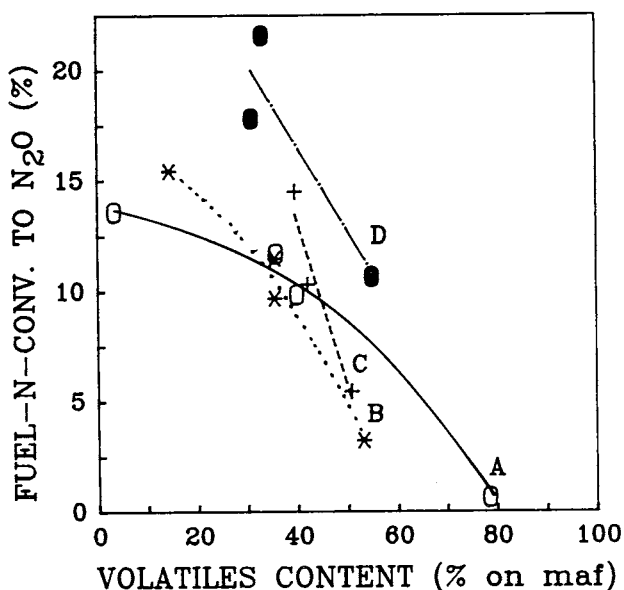


Figure 11 Influence of volatile matter of fuel on conversion of fuel-N to N<sub>2</sub>O during combustion in CFB reactors. A, B, C, D, see Table 6

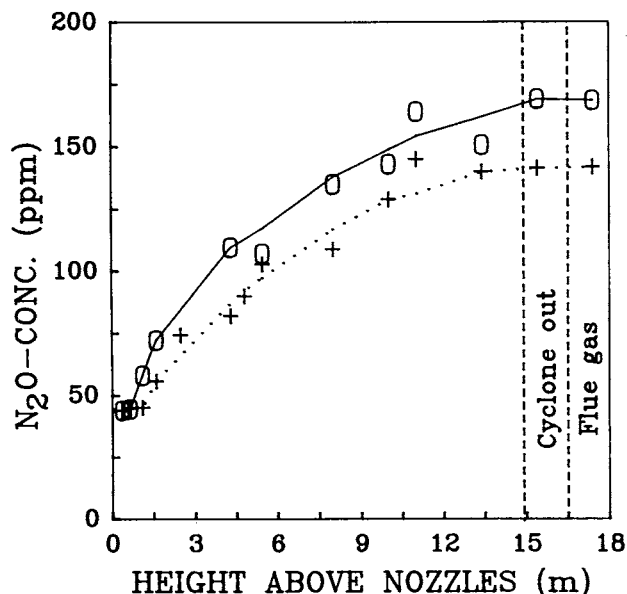


Figure 12 N<sub>2</sub>O concentration profiles at centre of combustion chamber for two different heights of secondary air supply: O, 2.2 m; +, 3.8 m. Adapted from ref. 33

of reactor. This could have led to overestimation of the reduction in the bottom of the bed, where some large particles should have been present.

In spite of this problem, some quantitative estimates can be made. Thermal decomposition of N<sub>2</sub>O forms a lower limit of reduction. The straight-line relation of thermal decomposition to height, shown in Figure 10, is an expression of residence time in the almost isothermal combustor. The contribution of bed material, consisting mostly of silica sand, is probably small in the present tests and reasonably well represented by the quartz sand data of Santala *et al.*<sup>20</sup>. The difference between these data and the measured values should then be the reduction by char and volatiles. The proportionately greater reduction in the bottom of the combustor for all three fuels could represent a contribution from the higher concentrations of volatiles and char in this region (cf. Tables 3 and 4). The tables also show that the concentration of products from the volatiles is low over the entire combustion chamber in the case of coke. Thus the situation with coke can be regarded as being dominated by reduction by char, and the difference between this case and those of the other fuels gives a rough estimate of a minimum contribution to N<sub>2</sub>O reduction by volatiles combustion. With wood the contribution of volatiles is probably larger, considering the small amount of char in this case. Furthermore, it can be stated that in the upper part of the combustor and in the cyclone, where the concentration of char is small, the reduction by volatiles becomes more important than that by char, illustrated by the still large reduction at 12 m in Figure 7 during wood combustion compared with coke combustion. The residual combustion of volatiles in the cyclone in the case of wood clearly plays a role; the reduction of the N<sub>2</sub>O injected at the entrance of the cyclone is 40%.

*Interpretation of the vertical concentration profile of N<sub>2</sub>O*

The fall in N<sub>2</sub>O reduction with increasing height of injection into the combustion chamber can be used to



explain the N<sub>2</sub>O concentration profile measured during combustion of bituminous coal in the same boiler<sup>33</sup>. It was found that the N<sub>2</sub>O concentration in the combustion chamber increased with height: *Figure 12*. Using the present data, this behaviour can be explained: the formation of N<sub>2</sub>O in the bottom zone of the combustion chamber is high, but its contribution to the emission of N<sub>2</sub>O is low, owing to the high reduction in this part of the combustion chamber. The smaller reduction of the N<sub>2</sub>O produced at higher levels leads to the conclusion that formation of N<sub>2</sub>O in the upper part of the combustion chamber becomes more important for the emission than is formation in the bottom zone.

## CONCLUSIONS

1. The combustion of low-volatile fuels leads to a smaller reduction of added N<sub>2</sub>O, compared with fuels of higher volatile matter.
2. The combustion of low-volatile fuels in a CFB boiler leads to the highest conversion of fuel-nitrogen to N<sub>2</sub>O. This is accentuated by the smaller reduction of N<sub>2</sub>O by low-volatile than high-volatile fuels.
3. The large reduction of the added N<sub>2</sub>O in the case of wood combustion implies that the homogeneous reactions involving radicals, reactions (R1) and (R2), are more important for N<sub>2</sub>O reduction than are large quantities of low-reactive char as in coke combustion.
4. The smaller reduction of the added N<sub>2</sub>O at higher levels in the combustion chamber explains the observed increase in N<sub>2</sub>O concentration with height.
5. The available laboratory data on N<sub>2</sub>O reduction are still not accurate enough for reliable predictions of the influence of bed material and char on the reduction of N<sub>2</sub>O in a CFB combustion chamber.

## ACKNOWLEDGEMENTS

This work was supported financially by the Swedish National and Technical Board for Industrial Development (NUTEK). The additional fuel costs due to fuel taxes and special fuel requirements, and the cost of the N<sub>2</sub>O added, were paid with support from the Swedish Energy Development Corporation (SEU) and Kvaerner Generator AB.

## REFERENCES

- 1 Mann, M. D., Collings, M. E. and Botros, P. E. *Prog. Energy Combust. Sci.* 1992, **18**, 447
- 2 'Fifth International Workshop on Nitrous Oxide Emissions', NIRE/IFP/EPA/SCEJ, Tsukuba, Japan, 1992
- 3 Hayhurst, A. N. and Lawrence, A. D. *Prog. Energy Combust. Sci.* 1992, **18**, 529
- 4 Wójtowicz, M. A., Pels, J. R. and Moulijn, J. A. *Fuel Process. Technol.* 1993, **34**, 1
- 5 Åmand, L.-E. and Leckner, B. *Energy Fuels* 1993, **7**, 1097
- 6 Miller, J. A. and Bowman, C. T. *Prog. Energy Combust. Sci.* 1989, **15**, 287
- 7 Kramlich, J. C., Cole, J. A., McCarthy, J. M., Lanier, W. S. and McSorley, J. A. *Combust. Flame* 1989, **77**, 375
- 8 Kilpinen, P. and Hupa, M. *Combust. Flame* 1991, **85**, 94
- 9 Hulgaard, T., Glarborg, P. and Dam-Johansen, K. In 'Eleventh International Conference on Fluidized Bed Combustion' (Ed. E. J. Anthony), American Society of Mechanical Engineers, New York, 1991, pp. 991-998
- 10 Hulgaard, T. 'Nitrous Oxide from Combustion', Dr Thesis, Dept of Chemical Engineering, Technical University of Denmark, 1991
- 11 Johnsson, J.-E., Glarborg, P. and Dam-Johansen, K. In 'Twenty-Fourth Symposium (International) on Combustion', The Combustion Institute, Pittsburgh, 1992, pp. 917-923
- 12 Iisa, K., Salokoski, P. and Hupa, M. In 'Eleventh International Conference on Fluidized Bed Combustion' (Ed. E. J. Anthony), American Society of Mechanical Engineers, New York, 1991, pp. 1027-1033
- 13 Miettinen, H., Strömberg, D. and Lindquist, O. In 'Eleventh International Conference on Fluidized Bed Combustion' (Ed. E. J. Anthony), American Society of Mechanical Engineers, New York, 1991, pp. 999-1003
- 14 Aho, M. J., Rantanen, J. T. and Linna, V. L. *Fuel* 1990, **69**, 957
- 15 De Soete, G. G. in 'Twenty-Third Symposium (International) on Combustion', The Combustion Institute, Pittsburgh, 1990, pp. 1257-1264
- 16 Moritomi, H. and Suzuki, Y. in Proceedings of the Seventh Engineering Foundation Conference on Fluidization (Eds O. E. Potter and D. J. Nicklin), Engineering Foundation, New York, 1992, pp. 495-503
- 17 Suzuki, Y., Moritomi, H. and Kido, N. In Proceedings of the Fourth SCEJ Symposium on Circulating Fluidized Beds, Chemical Engineering Society of Japan, Tokyo, 1991, pp. 125-133
- 18 Gulyurtlu, I., Costa, M. R., Esparteiro, H. and Cabrita, I. In Proceedings of the Fifth International Fluidized Bed Combustion Conference (The Institute of Energy), Adam Hilger, Bristol, 1991, pp. 201-212
- 19 Naruse, I., Imanari, M., Koizumi, K. and Ohtake, K. In Proceedings of the Fifth International Workshop on Nitrous Oxide Emissions, NIRE/IFP/EPA/SCEJ, Tsukuba, Japan, 1992, pp. 8-2-1 to 8-2-8
- 20 Santala, P., Iisa, K. and Hupa, M. 'Catalytic Destruction of N<sub>2</sub>O in a Fixed Bed Laboratory Reactor', Report 90-6, Åbo Akademi, Finland
- 21 Wójtowicz, M. A., Pels, J. R. and Moulijn, J. A. In Proceedings of the 1991 International Conference on Coal Science, Butterworth-Heinemann, Oxford, 1991, pp. 452-455
- 22 Klein, M., Köser, H. and Rotzoll, G. In Proceedings of the Fifth International Workshop on Nitrous Oxide Emissions, NIRE/IFP/EPA/SCEJ, Tsukuba, Japan, 1992, pp. 5-1-1 to 5-1-8
- 23 Kimura, N. In Proceedings of the Fifth International Workshop on Nitrous Oxide Emissions, NIRE/IFP/EPA/SCEJ, Tsukuba, Japan, 1992, pp. 8-3-1 to 8-3-9
- 24 Khan, T., Lee, Y. Y. and Young, L. In Proceedings of the 1991 Joint Symposium on Stationary Combustion NO<sub>x</sub> Control, EPRI and EPA, Washington, DC, 1991
- 25 De Soete, G. G. In Proceedings of the Fifth International Workshop on Nitrous Oxide Emissions, NIRE/IFP/EPA/SCEJ, Tsukuba, Japan, 1992, pp. K1-4-1 to K1-4-24
- 26 Johnsson, J.-E. Paper to Twenty-Third International Energy Agency Meeting on Atmospheric Fluidized Bed Combustion, Florence, 1991
- 27 Leckner, B. and Åmand, L.-E. Paper to Joint Meeting of the French, Italian and Swedish Sections of the Combustion Institute, Associazione Sezione Italiana del Combustion Institute, Capri, 1992, Lecture V-1
- 28 Åmand, L.-E. and Leckner, B. In 'Twenty-Fourth Symposium (International) on Combustion', The Combustion Institute, Pittsburgh, 1992, pp. 1407-1414
- 29 Åmand, L.-E. and Leckner, B. *Combust. Flame* 1991, **84**, 181
- 30 Moritomi, H., Suzuki, Y., Kido, N. and Ogisu, Y. In 'Eleventh International Conference on Fluidized Bed Combustion' (Ed. E. J. Anthony), American Society of Mechanical Engineers, New York, 1991, pp. 1005-1013
- 31 Wójtowicz, M. A., Oude Lohuis, J. A., Tromp, P. J. J. and Moulijn, J. A. In 'Eleventh International Conference on Fluidized Bed Combustion' (Ed. E. J. Anthony), American Society of Mechanical Engineers, New York, 1991, pp. 1013-1020
- 32 Hiltunen, M., Kilpinen, P., Hupa, M. and Lee, Y. Y. In 'Eleventh International Conference on Fluidized Bed Combustion' (Ed. E. J. Anthony), American Society of Mechanical Engineers, New York, 1991, pp. 687-694
- 33 Åmand, L.-E., Leckner, B. and Andersson, S. *Energy Fuels* 1991, **5**, 815